International Journal of Engineering

J o u r n a l   H o m e p a g e :   w w w . i j e . i r

Micro-particles Transport and Deposition in Realistic Geometry of Human upper Airways

B. Tavakoli [a], O. Abouali [a,*], M. H. Bagheri [b], M. Yazdi [c], G. Ahmadi [d]

[a] *School of Mechanical Engineering, Shiraz University, Shiraz, Iran*
[b] *Medical Imaging Research Cenetr, Namazi Hospital, Shiraz, Iran*
[c] *School of Electrical and Computer Engineering, Shiraz University, Shiraz, Iran*
[d] *Department of Mechanical And Aeronautical Engineering, Clarkson University, Potsdam, US*

P A P E R I N F O	*A B S T R A C T*

The realistic geometry of human upper airways from the mouth to the end of the trachea was reconstructed by implementing the CT-Scan images of a male subject. A computational simulation was developed for analyzing the airflow in the airways. To capture the anisotropy of the inhaled airflow in the upper airways, the Reynolds stress transport turbulence model was used in these simulations. The inhalation rates of 15, 30 and 60 l/min which represented the resting, normal and active conditions of human, respectively were underlined. The transport and deposition of micro particles in the realistic model of human upper airways were studied. The transport of micro particles was analyzed using the Lagrangian particle trajectory approach. Since the mass fraction of inhaled particles was very small, one-way coupling assumption was used. That is, the airflow carries the particles, but particles do not affect the airflow condition. The predicted deposition fractions of the particles of different sizes in the upper airways were compared with the available experimental data to find good agreements. Comparison of the results of the deposition fraction obtained from the realistic model with the earlier simulations of the idealized geometry of the airways showed certain differences especially in regional depositions. Therefore, it was concluded that the realistic geometry must be used for more accurate evaluation of micro particle deposition rates especially for local and regional depositions.

1. INTRODUCTION

Understanding the transport and deposition of suspended particles in ambient air in human airways has attracted considerable attention due to the adverse health effects of air pollution. In addition, many therapeutic drugs are produced in the aerosols form with the intention of being administered to patient by inhalers for treatment of lung diseases and other illnesses. Knowledge of particle transport behavior in human respiratory system helps the physicians to properly assess the needed dosage for their patients [1- 3]. Thus, it is important to provide information on the deposition fraction and distribution of inhaled particles in different parts of the human airways, and for different rates of breathing. The breathing rate, however, varies depending on the level of physical activity. On the average, the breathing rate of adults at rest is about 15 l/min, during normal activity it reaches to about 30 l/min, and during vigorous sport activities the breathing rate is about 60 l/min.

The mechanisms of particle deposition in respiratory tract include impaction, gravitational sedimentation and diffusion [4]. Impaction is the dominant deposition mechanism for large particles, with diameters larger than a few micrometers, and for particles having relatively high velocity. On the other hand, diffusion is the dominant deposition mechanism for small size particles (of the order of a few nano-meters). Cheng et al. [5] made a cast of oral airway from a male adult cadaver. They presented their experimental data for deposition of micro-particles and compared their results with the numerical analysis of the deposition of particles in a 90° bending pipe. They found that the minimum dimension of the airway passage near the larynx/pharynx and the average cross sectional area of oral airways are important parameters affecting the particle deposition.

Corresponding Author Email: abouali@shirazu.ac.ir (O. Abouali)

Zhang and Kleinstreuer [6] compared their simulated airflow field using various two-equation turbulence models in a constricted conduit and concluded that the low-Reynolds type of k-ω model is most suitable for predicting the laminar-transitional-turbulent airflows. Zhang et al. [7] simulated the airflow field and micro-particle transport by LRN k-ω model employing a simplified form of the geometry proposed by Cheng et al. [5] for human oral airways. They showed that the turbulent flow appearing after the constriction in the glottis plays an important role on micro-particles deposition. The main limit of their work was the big difference of local deposition of the micro particles in comparison with experimental data of Cheng et al. [5]. Olsen et al. [8] showed that although the inhalation is a periodic process, the averaged steady flow accurately represents the conditions of the flow field during the respiration. The complex geometry of upper oral airways including oral cavity, pharynx, larynx, and trachea has the major effect on the amount and spatial distribution of deposited particles [5]. Li and Ahmadi [9], He and Ahmadi [10] and Tian and Ahmadi [11] showed that the turbulence models based on eddy viscosity hypothesis, could not accurately predict the particle deposition rate since the anisotropic feature of the turbulence intensity is ignored. Tavakoli et al. [12] studied the distribution and deposition of nano particles in an idealized geometry of human upper airways presented by Y. S. Cheng et al. [5] using the Reynolds stress turbulence mode.

The geometry of human upper airways is quite complicated and understanding the behavior of particle motion in such geometries is rather challenging. Vos et al. [13] implemented CT_Scan images for constructing their model. They studied the airflow field and the effect of the shape of airways on Apnea/Hypopnea Syndrome. Jayaraju et al. [14] used a commercial software program to transfer the CT-Scan images to a 3D CAD geometry. They simulated the airflow and the distribution of the particles in sizes of 2 to 20 micrometers.

In this study, the inhaled airflow in human upper airways is simulated using the Reynolds stress transport turbulence model in order to capture the anisotropic feature of the flow field. Furthermore, the distributions of micro particles in the different parts of the upper airways are predicted using the Eulerian-Lagrangian approach and assuming one way coupling.

2. GOVERNING EQUATIONS

2. 1. Gas Phase
In this study an incompressible, steady airflow in the airway is simulated. The ensemble averaged continuity and momentum equations are:

$$\frac{\partial \bar{u}_i}{\partial x_i} = 0 \tag{1}$$

$$\frac{D\bar{u}_i}{Dt} = -\frac{\partial p}{\partial x_i} + \upsilon \frac{\partial^2 \bar{u}_i}{\partial x_j \partial x_j} - \frac{\partial}{\partial x_j} \overline{u'_i u'_j} \tag{2}$$

where, the Cartesian tensor notation is used, and the $\overline{u'_i u'_j}$ is the Reynolds turbulence stress tensor. In order to model the turbulence stresses, the k-ω turbulence model in addition to the Reynolds stress transport model were used in the analysis. The stress transport models of LRR (Launder, Reece and Rodi) is given as

$$\frac{D}{Dt}\left(\rho \overline{u'_i u'_j}\right) = d_{ij} + P_{ij} - \varepsilon_{ij} + \phi_{ij} \tag{3}$$

The terms on the right hand side of Equation (3) are diffusion, Production, dissipation and the pressure/strain terms, respectively. The details model of these terms may be found in some literatures [16]. The transport equation for the turbulence energy dissipation in LRR model is given as:

$$\rho \frac{D\varepsilon}{Dt} = \frac{\partial}{\partial x_j}\left[\left(\mu + \frac{\mu_t}{\sigma_\varepsilon}\right)\frac{\partial \varepsilon}{\partial x_j}\right] + C_{\varepsilon 1}\frac{1}{2}\left[P_{ii} + C_{\varepsilon 3}G_{ii}\right]\frac{\varepsilon}{k} - C_{\varepsilon 2}\rho\frac{\varepsilon^2}{k} \tag{4}$$

where, C_{si} are the constant coefficients.

2. 2. Particle Phase
The drag force is the most important force acting on the particles. Particles equation of motion is then given as

$$\frac{du_i^p}{dt} = \frac{3\mu C_D \operatorname{Re}_p}{4\rho_p d_p^2 C_c}\left(u_i - u_i^p\right) + g \tag{5}$$

where the particle Reynolds number is defined as

$$\operatorname{Re}_p = \rho\left|u_j - u_j^p\right|d / \mu \tag{6}$$

Here, C_c is the Cunningham slip correction factor. The drag coefficient is given as

$$C_D = \frac{24}{\operatorname{Re}_p}\left(1 + 0.15 \operatorname{Re}_p^{0.687}\right) \tag{7}$$

The corresponding deposition fraction of micro-particles is defined as

$$DF = \frac{\text{Number of deposited particles on the walls}}{\text{Number of particles entered to the mouth}} \tag{8}$$

3. THE MODEL DESCRIPTION AND THE NUMERICAL SCHEME

The 3D geometry of human upper airways is reconstructed in four steps. At first step, CT-Scan images with proper resolutions from one male volunteer with normal and healthy respiratory system were taken. Figure 1 shows the mid sagittal plane of the volunteer upper airways images.

Figure 1. CT-Scan image of the upper airways (Sagital view).

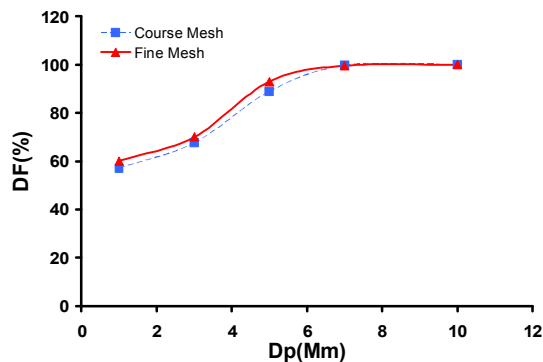**Figure 2.** Reconstructed 3D geometry of the upper airway.

Figure 3. Comparison of the deposition of micro particles for two different grid sizes.
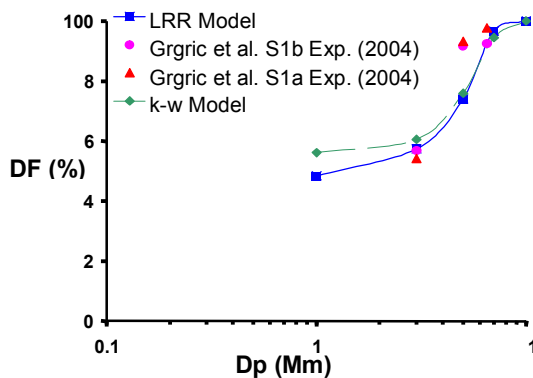

Figure 4. Comparison of the present numerical results with the experimental data for deposition fraction of micro particles in flow rate of 60 l/min.

In addition, using MTALAB software, CT-Scan images are processed and the boundary coordinates of the walls of the upper airways are identified. Then the outcome of the image processing is imported into CATIA software. As it is depicted in Figure 2, the 3D geometry of the passage in CAD format is reconstructed. Finally, using multi block method, a numerical grid for the CFD analysis is generated with GAMBIT software. The grid study was conducted to find a solution independent of grid size. Figure 3 shows a comparison between two grid sizes. As the figure shows, the deposition fraction of mirco particles are nearly the same for both grid sizes. It means that the fine grid size used in this study is appropriate. The fine grid has 1,700,000 cells. The numerical simulation is performed by applying 4 parallel computers taking 120 h of CPU time for each case.

4. RESULTS AND DISCUSSION

At first the present numerical model was validated by comparing the numerical results of micro particles deposition fraction with the available experimental data. Two different turbulence models were used in the numerical model. The LRR model (which is a Reynolds stress model) shows a better agreement compared with k-ω model. The an-isotropic behavior of the Reynolds stress tensor components can be predicted by the Reynolds stress model. The numerical results are generally in good agreement with the experimental data of Grgric et al. [17]. Grgric et al. [17] have two different case studies; S1a and S1b refer to two sets of intrasubject geometric configurations of mouth and throat realistic models obtained from MRI scans. It should be noted that the available experimental data were for 90 l/min of volume flow rate.

Figures 5-7 show local deposition fraction of micro-particles in the mouth, pharynx, larynx and trachea for the flow rates of 15, 30 and 60 l/min. The particles with smaller diameters penetrate deeper into the upper airways and get into larynx and trachea, while larger particles are captured in upper parts including mouth and pharynx. As depicted in Figures 5-7, the deposition of larger micro particles are dominant in the mouth region, which was seen before in the experimental data of Cheng et al. [5]. While the results of numerical simulation using idealized geometry of upper airways [7, 12] were not able to present the same trend.

The total deposition fraction of micro particles versus particles diameter and flow rates are shown in Figure 8. By increasing the flow rates and the particles sizes, the deposition fraction of the micro-particles increase too. For large particles, the deposition is mainly controlled by the impaction process. While the airflow suddenly changes the directions due to the bends in the
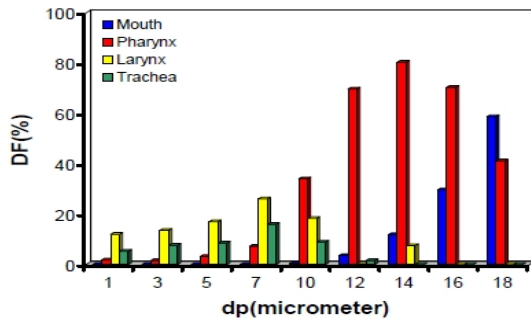
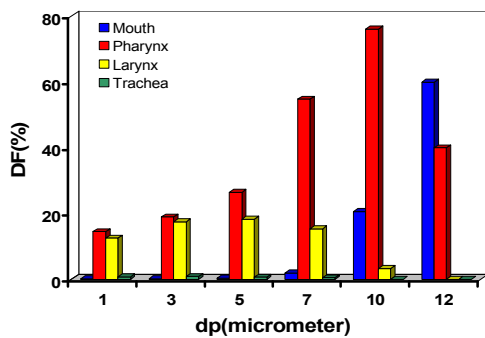**Figure 5.** Local deposition fraction of micro-particles for a breathing rate of 15 l/min.

Figure 6. Local deposition fraction of micro-particles for a breathing rate of 30 l/min.
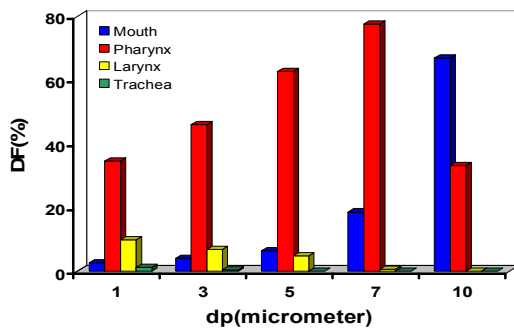

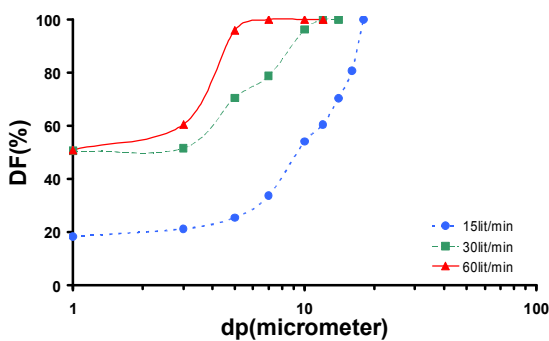**Figure 7.** Local deposition fraction of micro-particles for a breathing rate of 60 l/min.

Figure 8. Deposition fraction of micro particles in realistic geometry of human upper airways at different breathing rates.

Figure 9. Depositions pattern of 3, 7 and 16μm particles on the walls of the upper airways in the breathing rate of 15 l/min

upper airways, the large particles are not able to follow the streamlines. Therefore, the particles deviate from their streamlines and impact the walls of the upper airways.

Figures 9-11 show the pattern depositions of the 3, 7 and 16 μm particles in the realistic upper airways of the live person for 15, 30 and 60 l/min breathing rates, respectively. For breathing flow rate of 15 l/min, most of the 3 μm particles are trapped in the larynx and the inlet of the trachea. However, 16 μm particles are deposited in the pharynx and mouth regions mostly. Figure 10 shows that for the breathing flow rate of 30 l/min most of the 3 and 7 μm particles are filtered in the pharynx and in the inlet of the larynx. This is because of the higher inertia of the particles in this flow rate, which results in capturing the particles in complex geometry of the pharynx and the larynx inlet. All the 16 μm particles are trapped in the mouth region for the 30 l/min flow rate. In the 60 l/min breathing flow rate, as was expected, the high inertia of the particles resulted to the filtration at the upper parts of the airway. The mouth and the pharynx play an important role for this aim. It should be emphasized that the Figures 9-11 show the general trend of the deposition pattern in the realistic airway. For the clarity of the figures, only a few numbers of the particles were shown in the figures. The accurate percent of the particles deposition can be found from the bar charts shown in Figures 5-7.

Figures 12-14 show the cross flow velocity vectors as well as the distribution of 1 μm particles in different cross sections of the realistic geometry of upper airways for the 15 l/min breathing flow rate. The complex geometry of the oral airway with various bends and cross sections leade to the complex secondary flow patterns in the airway. This also makes the distribution of the mirco-particles variable versus their locations in

the upper oral airway. Although the flow field and distribution of particles are much different in various cross sections, these patterns are nearly the same for various flow rates in the similar cross sections. For sure

this trend is for very small micro particles such as 1μm particles which are more affected by the flow field in comparison with the larger micro particles.

Figure 10. Depositions pattern of 3, 7 and 16μm particles on the walls of the upper airways in the breathing rate of 30 l/min.

Figure 11. Depositions pattern of 3, 7 and 16μm particles on the walls of the upper airways in the breathing rate of 60 l/min.

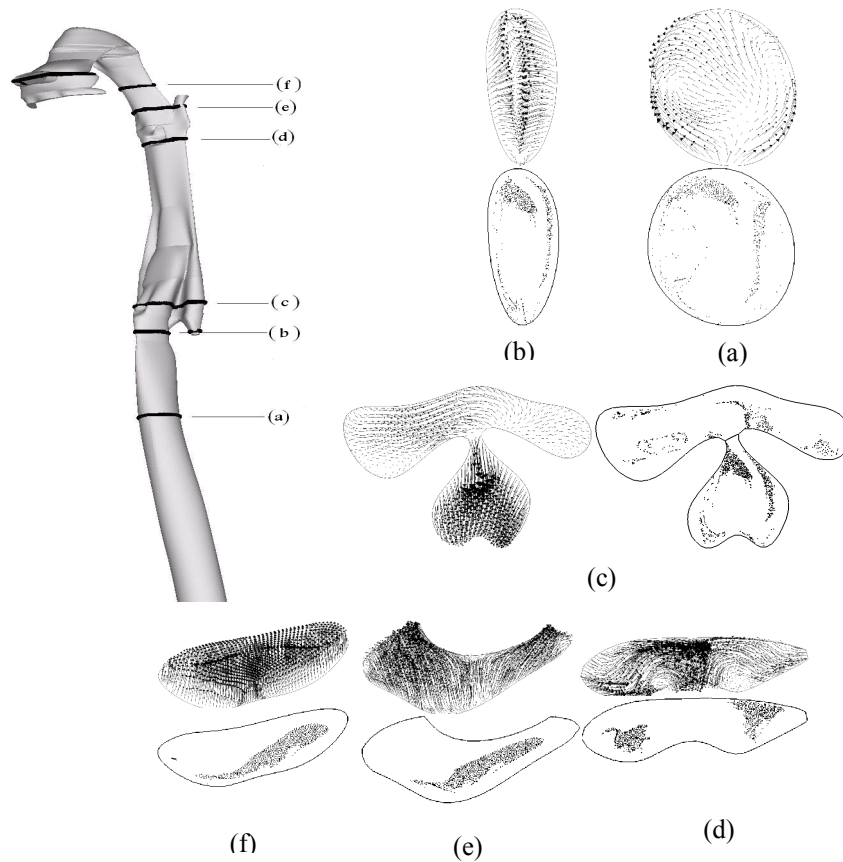**Figure 12.** Cross flow velocity vectors and the distribution of 1 μm micro particles for 15 l/min flow rate in cross sections of (a) Upper part of trachea, (b) Glottis, (c) Exit of larynx, (d) Inlet of larynx, (e) and (f) Cross sections of pharynx.

Figure 13. Cross flow velocity vectors and distribution of 1 μm micro particles for 30 l/min flow rate in cross sections of (a) Upper part of trachea, (b) Glottis, (c) Exit of larynx, (d) Inlet of larynx, (e) and (f) Cross sections of pharynx.
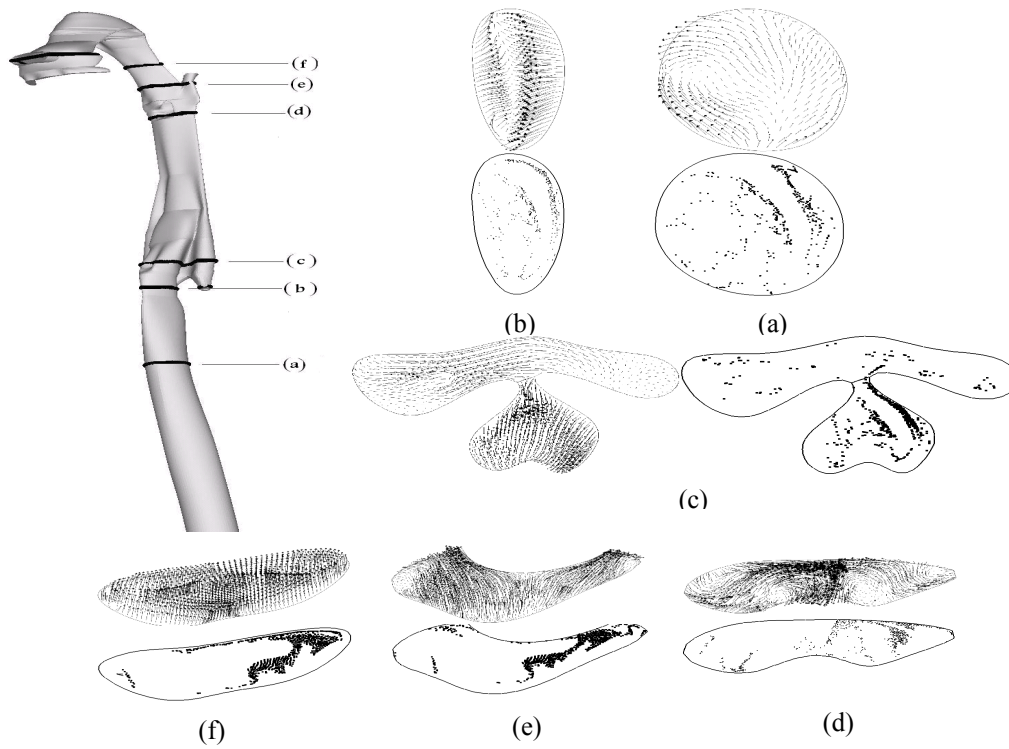
Figure 14. Cross flow velocity vectors and distribution of 1 μm micro particles for 60 l/min flow rate in cross sections of (a) Upper part of trachea, (b) Glottis, (c) Exit of larynx, (d) Inlet of larynx, (e) and (f) Cross sections of pharynx.
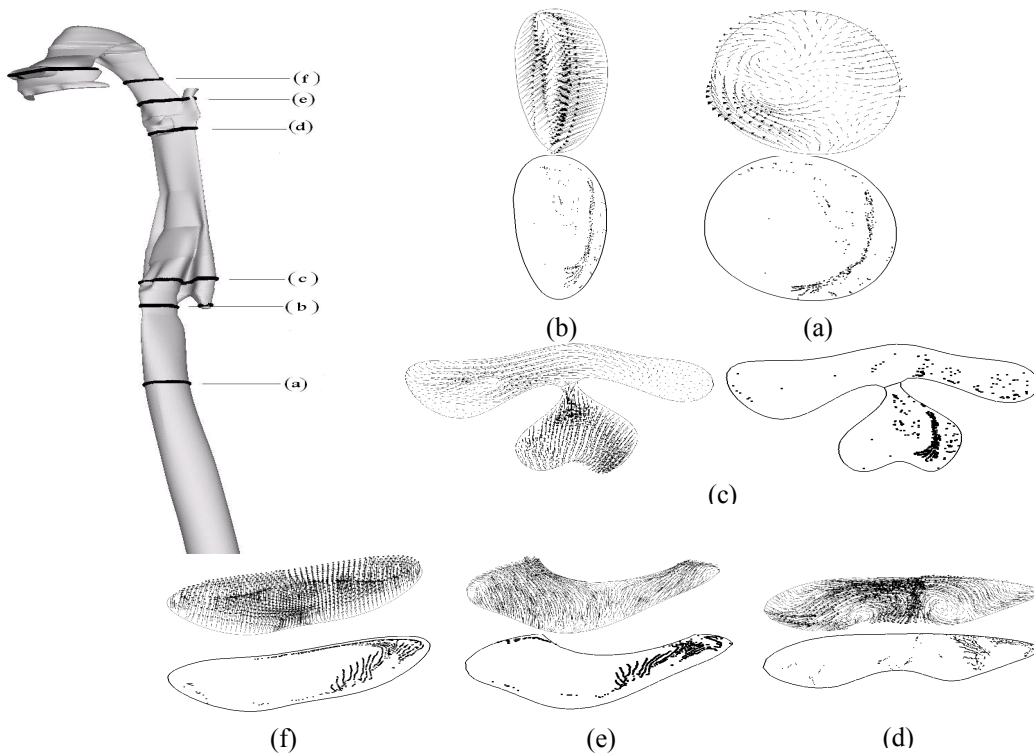
5. CONCLUSION

In this paper the flow field as well as the motion and deposition of the particles in micro sizes in a realistic geometry of upper airways, belonged to a live adult person, was investigated. Analysis of the local deposition fraction of particles shows that the particle deposition rate strongly depends on the flow field and the geometry of human upper airways. The dominant mechanism of micro-particles deposition is the impaction process. Consequently, the micro-particles deposition increased when the particles diameter or the flow rate increased. The results of the simulation in real geometry are in a good agreement with the experimental data, which shows that the mouth part has the most important role in filtration of the large micro particles. This important result solved the limitation of most of earlier researches, which used an idealized geometry of upper airways and it shows that the accurate prediction of local depositions of micro particles is only possible with modeling a realistic geometry.

6. REFERENCES

1. Frampton, M.W., "Systemic and cardiovascular effects of airway injury and inflammation: ultrafine particle exposure in humans", *Environment and Health Perspectives,* Vol. 109, (2001), 529–532.

2. Donaldson, K., Stone, V., Gilmour, P.S., Brown, D.M., & Macnee, W., "Ultrafine particles: mechanisms of lung injury", *Philosophical Transactions of the Royal Society,* Vol. 358, (2000), 2741–2749.

3. Oberdörster, G., "Pulmonary effects of inhaled ultrafine particles", *International Archives Occupational and Environmental Heath,* Vol. 74, (2001), 1–8.

4. Hinds, W.C. "Aerosol technology", John Wiley and sons, 2nd edition, (1999).

5. Cheng, Y.S., Zhou, Y. and Chen, B.T., "Particle deposition in a cast of human oral airways", *Aerosol Science and Technology,* Vol. 31, (1999), 286-300.

6. Zhang, Z. and Kleinstreuer, C., "Low-Reynolds-number turbulent flows in locally constricted conduits: A Comparison Study", *AIAA Journal,* Vol. 41, (2003), 831-840.

7. Zhang, Z., Kleinstreuer, C. and Kim, C.S., "Micro-particle transport and deposition in a human oral airway model", *Aerosol Science*, Vol. 33, (2002), 1635–1652.

8. Olsen, D.E. Sudlow, M. F. Horsfield, K. and Filey, G. P., "Convective patterns of flow during inspiration", *Archives of Internal Medicine,* Vol. 131, (1973), 51-57.

9. Li, A. and Ahmadi, G., "Computer simulation of particle deposition in upper tracheobronchial tree", *Aerosol Science and Technology,* Vol. 23, (1995), 201–223.

10. He C., and Ahmadi, G., "Particle deposition in a nearly developed turbulent duct flow with electrophoresis", *Aerosol Science and Technology,* Vol. 30, (1999), 739–758.

11. Tian, L. and Ahmadi, G., "Particle deposition in turbulent duct flows – comparisons of different model predictions", *Journal of Aerosol Science,* Vol. 38, (2007), 377–397.

12. Tavakoli, B., Abouali, O. and Ahmadi, G., "Numerical simulation of nano-particles deposition in human upper oral airways", *International Conference on multiphase Flow,* Leipzig, Germany, (2007).

13. Vos, W., De Backer, J., Dedolder, A., Vanderveken, O., Verhulst, S., Salgado, R., Germonpre, P., Partoens, B., Wuyts, F., Parizel, P. and De Backer, W., "Correlation between severity of sleep apnea and upper airway morphology based on advanced anatomical and functional imaging", *Biomedical. Biomechanics,* Vol. 40, (2007), 2207-2213.

14. Jayaraju, S.T.; Brouns, M.;Verbanck, S. and Lacor, C.; "Fluid flow and particle deposition analysis in a realistic extrathoracic airway model using unstructured grids", *Journal of Aerosol Science,* Vol. 38, No. 5, (2007), 494-508.

15. Launder, B.E., Reece, G.J. and Rodi, W., "progress in the development of a Reynolds-stress turbulence closure", *Fluid Mechanics,* Vol. 68, (1975), 537-566.

16. ANSYS Inc. "FLUENT 6.1".

17. Grgric, B., Finlay, W.H., Burnell, P.K.P. and Heenan, A.F., "In vitro intersubject and intrasubject deposition measurements in realistic mouth-throat geometries", *Journal of Aerosol Science and Technology,* Vol. 35, (2004), 1025-1040.

Micro-particles Transport and Deposition in Realistic Geometry of Human upper Airways

B. Tavakoli [a], O. Abouali [a], M. H. Bagheri [b], M. Yazdi [c], G. Ahmadi [d]

[a] *School of Mechanical Engineering, Shiraz University, Shiraz, Iran*
[b] *Medical Imaging Research Cenetr, Namazi Hospital, Shiraz, Iran*
[c] *School of Electrical and Computer Engineering, Shiraz University, Shiraz, Iran*
[d] *Department of Mechanical And Aeronautical Engineering, Clarkson University, Potsdam, US*

چکیده

هندسه واقعی مجاری تنفسی بالایی متعلق به یک مرد بالغ از دهان تا انتهای نای در محل دو شاخه شدن نای در شش با استفاده از تصاویر CT-Scan بازسازی شده است. جریان متلاطم هوا در مجاری تنفسی شبیه سازی شده است. برای اینکه مشخصات غیر ایزوترویک هوای دمیده شده به مجاری تنفسی در شبیه سازی لحاظ شود از مدل تنش رینولدز استفاده شده است. سه دبی حجمی هوای دمیده شده مورد بررسی قرار گرفته است که شامل ۱۵ l/min، ۳۰ l/min و ۶۰ l/min است و به ترتیب نماینده سه وضعیت استراحت، فعالیت روزمره و فعالیت ورزشی هستند. جابجایی و نشست ذرات در مدل واقعی مجاری تنفسی مورد بررسی قرار گرفته است. جابجایی ذرات توسط مدل لاگرانژی مورد مطالعه قرار گرفته است. از آنجا که نسبت جرمی ذرات به هوای دمیده شده بسیار اندک است از مدل یکطرفه، که در آن تنها تاثیر جریان هوا بر ذرات در نظر گرفته می شود و از تاثیر ذرات بر جریان چشم پوشی می شود، استفاده شده است. مقایسه درصد نشست ذرات حاصل از شبیه سازی عددی با داده های آزمایشی موجود نشان می دهد که پیش بینی عددی سازگار با نتایج آزمایشگاهی است. به علاوه، درصد نشست ذرات در مدل واقعی مجاری تنفسی با شبیه سازی های مشابه ولی در مدلهای ساده سازی شده از هندسه مجاری تنفسی با یکدیگر مقایسه شده اند. به خصوص تفاوت شایان توجهی در درصد نشست موضعی ذرات در انتهای دهان و ابتدای نای بین مدل واقعی و ساده سازی شده از مجاری تنفسی دیده می شود که اهمیت شبیه سازی انتقال ذرات در مدل واقعی از هندسه مجاری تنفسی را نشان می دهد.

doi: *10.5829/idosi.ije.2012.25.04a.03*